Nonlinear Tolerant Sphere Shaping with Dispersion-Aware Sequence Selection

Jingtian Liu
Télécom Paris
Institut Polytechnique de Paris
Palaiseau, FRANCE
jingtian.liu@telecom-paris.fr

Élie Awwad
Télécom Paris
Institut Polytechnique de Paris
Palaiseau, FRANCE
elie.awwad@telecom-paris.fr

Yves Jaouën
Télécom Paris
Institut Polytechnique de Paris
Palaiseau, FRANCE
yves.jaouen@telecom-paris.fr

***Abstract*—Energy dispersion index of dispersed sequences (D-EDI) with sequence selection demonstrates nonlinear shaping gains of 0.3 and 0.03 bits/4D-symbol over single-span and multi-span links respectively against conventional sphere shaping.**

***Index Terms*—Probabilistic constellation shaping, sequence selection, fiber non-linearity, coherent transmission systems.**

I. Introduction

Probabilistic constellation shaping (PCS) has shown remarkable performance when applied over linear AWGN channels. Various distribution matching (DM) techniques were proposed to implement PCS, of which we mention enumerative sphere shaping (ESS) [1] and constant composition distribution matching (CCDM) [2]. However, PCS sequences may experience performance degradation under the influence of the nonlinear Kerr effect in optical fibers [3]. Recent efforts have been directed at enhancing the nonlinear performance of PCS schemes. While some approaches focused on constraining the 1D amplitude variance such as the band-limited ESS (B-ESS) [4], or the kurtosis (K-ESS) [5], other works considered limiting the 2D (I and Q parts of a polarization tributary) energy dispersion index (EDI) of CCDM schemes [6], or implemented a perturbation-model based sequence selection (SS) ESS [7], or limited the 4D (I and Q signals of two polarization states) energy variations [8]. However, all used metrics only considered power variations of the sequence at the transmitter side and ignored the impact of the propagation channel, and in particular of dispersion, on the generation of Kerr-induced nonlinear interference (NLI). Hence, the additional nonlinear gains of the new schemes were mostly achieved over single-span systems. A recent work in [9] showed that a sign-dependent metric is necessary to achieve gains over long-haul transmission using sequence selection (SS). Knowing the signs in 1D, or equivalently the phases of the 2D symbols, and applying a propagation-aware metric for SS can lead to higher nonlinear gains. In this work, we propose a novel sign-dependent metric, the EDI of sequences including dispersion, named D-EDI. By using EDI and D-EDI as metrics for SS, we define the E-SS and D-SS schemes respectively, and validate their performance over single-span and multi-span links.

Work funded by Huawei Technologies France. We thank Hartmut Hafermann and Yann Frignac for fruitful discussions.

II. E-SS and D-SS design

The basic idea is inspired from the list-CCDM [6]. In Fig. 1, the input bits to a 1D ESS distribution matcher (DM), that generates a block of l amplitudes, are composed of $k-\nu$ information bits and ν prefix flipping bits. Altering the ν prefix flipping bits can cause pronounced changes in the sequences' indices during the ESS encoding process. Such changes are reflected as considerable alterations in the amplitudes across the block. Conveniently, these flipping bits are discarded after the decoding process at the receiver side. We may also cascade the outputs of n 1D-DMs sequentially in time to generate longer sequences and perform selection on them. Then, the ln amplitudes are mapped to $\frac{ln}{4}$ 4D quadrature-and-amplitude-modulated (QAM) symbols. E-SS uses EDI [6] (a sign-independent metric) as a metric to select sequences, hence the assigned signs are not necessary. By changing the flip bits, and after 4D-mapping [10], $2^{\nu n}$ candidate sequences of length $\frac{ln}{4}$ 4D-QAM symbols enter the sequence selector (EDI calculator), and the sequence with the lowest 4D-energy EDI is selected for transmission. For a larger performance gain over long-haul links, we propose D-SS based on D-EDI. This metric requires the knowledge of sign bits to compute the form of the sequence after propagation over an ideal dispersive-only fiber. The signs can be fixed through a multi-block FEC-independent sequence selection as done in [9] (lower right of Fig. 9). In the sequence selector, D-EDI is obtained by averaging the EDI values computed at multiple locations on an ideal dispersive fiber, with 1 sample per symbol, as shown in Fig. 1. For a single-span link, one may apply D-EDI by cutting the span into multiple sections and adding up EDIs computed over the first sections where the signal power is still high. In what follows, to limit the metric complexity for a single-span link, we add up two EDI values: the one computed from the sequence at the transmitter side and the one computed after propagation over L_{eff}, the effective length of the span. For a multi-span link of m_D spans of length L_D km each, we add up the EDIs computed at the beginning of each span.

III. Simulation setup and results

We conducted a performance evaluation of the E-SS and D-SS systems over Pol-Mux 64-QAM with a block length

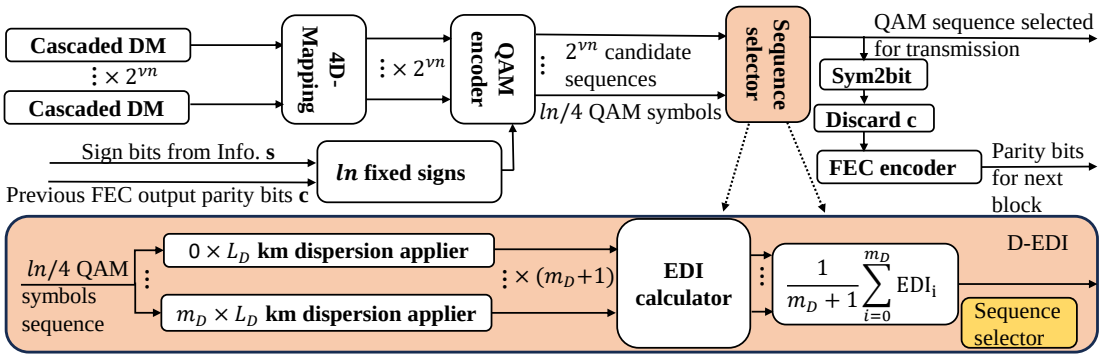

Fig. 1. Block diagram of D-SS in the PAS transmitter. EDI of dispersed sequences (D-EDI) is determined by averaging the calculated EDI at multiple locations along an ideal dispersive fiber. The dispersion is applied at 1 sample per symbol. EDI is a special case of D-EDI where $m_D = 0$. The sign bits are fixed through a multi-block FEC-independent sequence selection process as shown in [9].

$l = 108$ to match the conditions in [4], [5]. The transmitted signals consisted of 5 WDM channels with 50 GBaud (equivalently 600 Gbit/s raw bit rate) per channel. For all tested ESS schemes, we used a Low-Density Parity-Check (LDPC) code with a length of 64800 bits and $r_c = 5/6$ rate derived from the DVB-S2 standard. The achieved net rate is 8 bits/4D symbol. Channel spacing was set at 55 GHz and RRC pulse shaping was applied with a roll-off factor of 0.1. The standard single-mode fiber (SSMF) segments were modeled with an attenuation of $\alpha = 0.2$ dB/km, chromatic dispersion $D = 17\mathrm{ps/nm/km}$, $\mathrm{PMD} = 0.04\ \mathrm{ps}/\sqrt{\mathrm{km}}$, and a nonlinear parameter $\gamma = 1.3(\mathrm{W}\cdot\mathrm{km})^{-1}$ at 1550 nm. We first simulate a single-span transmission over 205 km as in [4], [5] without laser phase noise. Following propagation, the central channel underwent optical filtering, matched filtering, chromatic dispersion compensation, and genie-aided multiple-input-multiple-output (MIMO) channel equalization. Subsequently, we apply a fully-data-aided phase filter with an averaging window of 64 symbols to compensate for XPM-induced phase rotation as carrier phase recovery (CPR) [11]. Finally, we computed the $\mathrm{SNR_{elec}}$ from equalized constellations and the generalized mutual information (GMI) as Eq. (10) in [12].

First, we focus on the E-SS scheme. In Fig. $2(\mathrm{a}_1)$, we plot the $\mathrm{SNR_{elec}}$ for various EDI window lengths w (expressed in number of 4D symbols) used by the sequence selector. For this test, we used a single 1D DM ($n = 1$) and $\nu = 3$ flipping bits, and denote the scheme E-SS_1^3 (or in general $\text{E-SS}_\mathrm{n}^\nu$)[1]. This configuration allows us to select the most suitable sequence among eight candidates ($2^3 = 8$). We compute $\mathrm{SNR_{elec}}$ using equalized symbols after propagation over a single span with 9 dBm per channel, which is near the optimal power level. We see that, as w increases, the $\mathrm{SNR_{elec}}$ gradually declines. We find that a window length $w = 2$ yields the best performance, which is much lower than the channel memory (which is 76 when considering the total length of the span). Therefore, we proceed with $w = 2$ in subsequent single-span simulations. In Fig. $2(\mathrm{a}_2)$, we analyze the performance of E-SS by varying the number of sequentially cascaded DMs n, where each DM has ν flipping bits. A single DM with a block length $l = 108$ produces 27 4D-symbols after 4D-mapping. When cascading $n = 1, 2,$ or 4 DMs, the candidate sequence lengths will be $27, 54,$ and 108 respectively. We designate the number of tested candidate sequences per 4 DMs, i.e. per 108 4D-symbols, denoted $\mathrm{N_{S_{108}}}$, as a complexity metric. We choose 4 DMs as 4 is the least common multiple between the three studied values of n. To achieve a sequence of 108 4D symbols, the E-SS transmitter needs to be called $\frac{4}{n}$ times, resulting in $4, 2,$ and 1 calls for $n = 1, 2,$ and 4 cascaded DMs respectively. $\mathrm{N_{S_{108}}}$ is given by: $\mathrm{N_{S_{108}}} = \frac{4}{n}2^{\nu n}$. We see from Fig. 2 (a_2) that, as $\mathrm{N_{S_{108}}}$ increases, $\mathrm{SNR_{elec}}$ also increases for $n = \{1, 2, 4\}$. However, as the number of flipping bits increases, the rate loss likewise increases. The maximum GMI is hence attained when achieving a trade-off between rate loss and nonlinear gain. Specifically, the largest GMI is achieved with a single 1D-DM at $\log_2(\mathrm{N_{S_{108}}}) = 5$ (32 candidate sequences), corresponding to the E-SS_1^3 configuration.

Next, we test the D-SS performance over the same single-span link. $n = 1$ and $\nu = 4$ (D-SS_1^4) yield the best GMI gains through a similar optimization as the one shown in Fig. $2(\mathrm{a}_2)$ for E-SS. In Fig. $2(\mathrm{b}_1)$, we show $\mathrm{SNR_{elec}}$ versus the launch power per channel for five ESS schemes. The D-SS, E-SS, band-limited ESS (B-ESS), and kurtosis-limited ESS (K-ESS) show respectively a 0.8, 0.6, 1, and 0.3 dB SNR gain at a power of 10 dBm compared to conventional ESS, and a 1 dB enhancement in the optimal launch power. In Fig. $2(\mathrm{b}_2)$, we show the results in terms of GMI per 4D symbol. The D-SS shows the best GMI. At 10 dBm, the GMI is increased by 0.15 bits/4D compared to the B-ESS, and by 0.3 bits/4D compared to conventional ESS. The E-SS shows a 0.1 bits/4D gain (resp. 0.2 bits/4D) compared to the B-ESS (resp. conventional ESS). E-SS and D-SS have almost the same linear performance as conventional ESS due to their limited rate loss. D-SS has a lower rate loss than B-ESS, 0.26 bits/4D compared to 0.5 bits/4D, and better nonlinear performance than E-SS. It surpasses B-ESS in both linear and nonlinear regimes. we don't see the rate loss because non-linear gains

[1]For an ESS system employing sequence selection based on either EDI or D-EDI and comprising n cascaded DMs, where each DM includes ν flipping bits, we name the scheme $\text{E-SS}_\mathrm{n}^\nu$ for the EDI-based approach, and $\text{D-SS}_\mathrm{n}^\nu$ for the D-EDI-based approach.

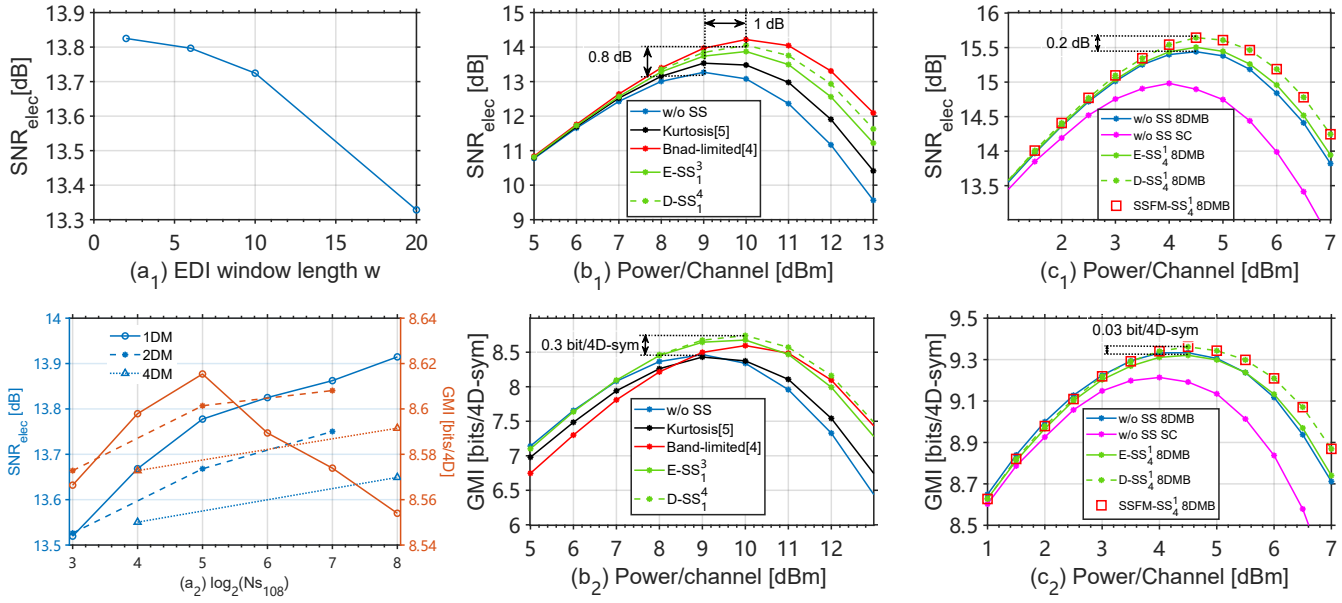

Fig. 2. $(\mathrm{a}_1, \mathrm{a}_2)$: Single-span optimization at 9 dBm, $(\mathrm{b}_1, \mathrm{b}_2)$: 205 km single-span, $(\mathrm{c}_1, \mathrm{c}_2)$: 30×80 km.

are already present before the optimum transmission point.

Now, we assess the potential gains of our schemes over higher baud rate long-haul links with digital-multi-band (DMB) signals known for their enhanced resilience to Kerr effects compared to single-carrier schemes [13]. In long-haul links, the impact of dispersion will translate into an interference of several hundreds of symbols, hence we cascade multiple 4D-DMs to get longer candidate sequences for an efficient selection that takes into account the impact of channel memory. As a first attempt, we propose to use $n = 4$ DMs, each having 1 flipping bit. We compare five single-wavelength schemes: ESS over DMB using 8 subcarriers (8DMB), ESS over a single carrier (SC), both E-SS_4^1 and D-SS_4^1 schemes with 8DMB, and 8DMB scheme along with sequence selection using a split-step Fourier method (SSFM) to model the propagation of each sequence through a noiseless link as in [9]. The baud rate is 110 Gbaud and the net bit rate is 880 Gbit/s over a 30×80 km SSMF link with 5 dB noise figure EDFA amplification. We use the same DSP blocks as the ones used in the previous scenario. In Fig. 2 (c_{1-2}), in comparison to the baseline conventional ESS over a single carrier, the 8DMB scheme shows a gain of 0.12 bits/4D through its rate optimization. The D-SS_4^1 shows a 0.2 dB increase in $\mathrm{SNR}_{\mathrm{elec}}$ and 0.03 bits/4D in GMI at a power of 4.5 dBm compared to ESS over 8DMB and it shows a 0.66 dB increase in $\mathrm{SNR}_{\mathrm{elec}}$ and 0.16 bits/4D in GMI at the optimal power compared to conventional ESS over SC. We can also see that, even if the E-SS_4^1 has a slight SNR gain, yet it does not counterbalance the rate loss, and there is no final gain in GMI. Remarkably, D-SS_4^1 performs on par with the ideal SSFM-based sequence selection method used in [9]. In conclusion, the sign-dependent-based D-SS scheme maintains the GMI advantage in both short-distance and long-haul distance transmissions.

IV. Conclusion

We proposed a sign-dependent metric, D-EDI, for sequence selection (SS) and we tested its performance along with ESS distribution matching. D-EDI-based SS (D-SS) achieved higher gains than state-of-the-art ESS schemes for both short-distance and long-haul links, at high baud rates, even when using a CPR algorithm. D-EDI, as a selection metric, has a lower complexity than SSFM-based selection [9]. These results confirm that sign-dependent and channel-aware metrics are necessary for efficient mitigation of nonlinear distortions in long-haul transmissions using sequence selection.

References

[1] Y. C. Gültekin *et al.*, "Enumerative sphere shaping for wireless communications with short packets," *T. Wireless Communications*, 2019.

[2] P. Schulte *et al.*, "Constant composition distribution matching," *IEEE Transactions on Information Theory*, 2015.

[3] T. Fehenberger *et al.*, "Analysis of nonlinear fiber interactions for finite-length constant-composition sequences," *JLT*, 2019.

[4] Y. C. Gültekin *et al.*, "Mitigating nonlinear interference by limiting energy variations in sphere shaping," in *OFC*, 2022.

[5] ——, "Kurtosis-limited sphere shaping for nonlinear interference noise reduction in optical channels," *JLT*, 2021.

[6] K. Wu *et al.*, "List-encoding CCDM: A nonlinearity-tolerant shaper aided by EDI," *JLT*, 2022.

[7] M. T. Askari *et al.*, "Probabilistic amplitude shaping and nonlinearity tolerance: Analysis and sequence selection method," *JLT*, 2023.

[8] J. Liu *et al.*, "Multi-dimensional Energy Limitation in Sphere Shaping for Nonlinear Interference Noise Mitigation," in *ACP*, 2023.

[9] S. Civelli *et al.*, "Sequence-selection-based constellation shaping for nonlinear channels," *JLT*, 2023.

[10] P. Skvortcov *et al.*, "Huffman-coded sphere shaping for extended-reach single-span links," *IEEE JSTQE*, 2021.

[11] T. Fehenberger *et al.*, "Compensation of XPM interference by blind tracking of the nonlinear phase." in *ECOC*, 2015.

[12] G. Böcherer, "Probabilistic signal shaping for bit-metric decoding," in *ISIT*. IEEE, 2014.

[13] J. Cho *et al.*, "Shaping lightwaves in time and frequency for optical fiber communication," *Nat. Commun.*, 2022.